Analysis of the Structure of Precipitation Patterns in New England

PAULINE M. AUSTIN AND ROBERT A. HOUZE, JR.

Dept. of Meteorology, Massachusetts Institute of Technology, Cambridge 02139

(Manuscript received 31 January 1972, in revised form 19 May 1972)

ABSTRACT

The studies presented here were undertaken to provide a specific and quantitative description of the precipitation patterns in New England storms. Basic data were quantitative radar observations and detailed raingage records.

Nine storms covering a wide range of synoptic and seasonal situations were subjected to systematic analysis. Also the general shape and configuration of the mesoscale rain areas in seventeen fully developed cyclones were observed.

The precipitation patterns, which at first glance appeared very dissimilar, turned out to be composed of subsynoptic-scale precipitation areas with rather clearly definable characteristics and behavior. Four distinct scales of precipitation areas have been recognized and described: synoptic areas which are larger that 10^4 km^2 and have a lifetime of one or several days; large mesoscale areas which range from 10^3–10^4 km^2 and last several hours; small mesoscale areas which cover 100–400 km^2 and last about an hour; and cells which are roughly 10 km^2 and often last only a few minutes, rarely as long as half an hour. In the cases which were analyzed every precipitation area of any of these scales contained one or several of each of the smaller sized precipitation areas. The motions and relative intensities of precipitation areas of the various scales also show a consistent pattern. The vertical location and depth of the layer containing cells varied greatly from one storm to another, but remained about the same within any particular storm.

The consistent occurrence of subsynoptic-scale rain areas with similar characteristics and behavior in a variety of precipitation patterns provides a means for describing the distribution of precipitation in any storm in a parameterized manner and also permits realistic modeling of storms for meteorological and hydrological studies.

1. Introduction

It has long been recognized that the intensity of precipitation is highly variable with significant changes often occurring over distances of less than a kilometer and time intervals on the order of a minute. Quantitative radar observations have shown that in all types of storms precipitation areas of many sizes, shapes and intensities occur simultaneously. Occasionally they exhibit a high degree of organization and form clearly recognizable patterns, as in "squall lines" or the spiral bands of hurricanes; more often, however, the patterns are chaotic in appearance and difficult to describe.

The studies presented here were undertaken to provide a specific and quantitative description of the precipitation patterns in New England storms with particular attention being directed to the characteristics of precipitation areas on the order of hundreds or a few thousands of square kilometers in extent. Precipitation areas in this size range are called mesoscale because they are intermediate between showers produced by cumulus convection and the broad regions of precipitation associated with warm frontal lifting in extratropical cyclones.

Characteristics and behavior of mesoscale precipitation areas are of interest not only in relation to precipitation mechanisms but also because their study offers a new approach to the exploration of subsynoptic-scale atmospheric motions. The nature of small-scale motions and their role within the larger scale phenomena are problems of considerable meteorological interest, but extremely difficult to analyze because direct measurement of most meteorological quantities would require a prohibitively dense network. The interpretation of precipitation patterns, which can be mapped with the necessary resolution, appears to be a possible method for investigating the small-scale atmospheric motions by developing kinematic models and comparing the computed distribution of precipitation with quantitative patterns obtained empirically.

2. Data and methods of analysis

Basic data for this study are scope displays from the three radars formerly or presently in operation in the Department of Meteorology at the Massachusetts Institute of Technology, and raingage records from the field station in West Concord, Mass., at a range of 28 km from the radar site.

Characteristics of the radars are summarized in Table 1. On all three radars the scopes display averaged, range-normalized, quantized signal intensity with

TABLE 1. Characteristics of weather radars at M.I.T.

	WR-66	SCR-615-B	AN/CPS-9
Wavelength (cm)	10.5	10.7	3.2
Beam width (degrees between half-power points)	1.3	3.0	1.0
Transmitted power (kW)	600	450	150

approximately 5 dB in each intensity interval. A complete sequence of intensity levels on the PPI (Plan Position Indicator) is photographed every 2–4 min. Approximately once an hour a number of observations of the vertical structure of the precipitation are taken on the RHI (Range Height Indicator). Calibration of the radars indicates a standard error of less than 1 dB in measured radar reflectivity of the storms and about 1.5 dB in deducing equivalent rainfall rates from the measured reflectivities. The 95% confidence limits for rainfall rates measured with the radars are approximately ± a factor of 2. Comparison with raingage data has demonstrated that this is a realistic estimate.

At the field station there are two tipping-bucket gages which have time resolutions of a few seconds in heavy rain and about a minute in light rain. The more sensitive one tips for every 0.01 mm of rain. These gages are regularly checked against each other and a weighing gage. Agreement is generally within 5%.

The radars and raingages were supplemented by conventional meteorological observations and by the hourly precipitation amounts for New England, published monthly by the National Weather Service. There are three radiosonde stations, 20 stations reporting hourly surface data, and 69 recording raingages within 200 km of the radar site.

Two studies have been conducted. In the first, eight storms were selected which had fairly large amounts of precipitation, good radar and raingage coverage, and represented a variety of seasonal and synoptic situations. In no case was there specific knowledge of the precipitation pattern in a storm before it was chosen, nor was any storm rejected because of the patterns it was found to contain. These eight storms are listed below, the storm of 8 July 1963 being divided into two portions as indicated.

To facilitate systematic analysis, precipitation areas were categorized according to their horizontal extent.

Date	Synoptic type
12 January 1963	Wave on stationary front
2 February 1963	Low moving from Great Lakes region
18 May 1963	Coastal low moving from southwest with overland low to west
9 June 1965	Air mass thunderstorms
8 July 1963 (PF)	Occluded front moving eastward from Great Lakes, prefrontal precipitation
8 July 1963 (F)	Same storm, frontal passage with squall line
29 August 1962	Coastal low (ex-hurricane)
17 September 1963	Wave on stationary front
6 December 1952	Cyclone approaching from southwest

Areas $\geqslant 10^4$ km^2 are referred to as *synoptic areas* since they are large enough to be delineated by the regular synoptic weather reports. They are not usually depicted to their full extent on the radars, and their locations and intensities were obtained primarily from maps of the hourly precipitation amounts. A small intense radar echo corresponding to an area on the order of 10 km^2 was assumed to represent a single cumulus convective element and is called a *cell*. A *mesoscale precipitation area* was specifically defined as being smaller than a synoptic area and larger than a cell, the limits being set, somewhat arbitrarily, at 50 km^2 and 10^4 km^2. Early in the analysis it became apparent that some of the precipitation patterns contained areas of two distinct sizes, both within the mesoscale range. These patterns showed several *small mesoscale areas* (SMSA's), from 50 to 1000 km^2 in size, located within *large mesoscale areas* (LMSA's) which were in the range 10^3 to 10^4 km^2. Fig. 1 is an example of two large mesoscale areas, each containing several small mesoscale areas and a number of cells. Mesoscale areas and cells were identified from the intensity level sequences on the radar PPI. They were tracked for their entire lifetimes or as long as the data permitted. It should be noted that, in general, the patterns are complex and irregular in structure so that from the observations taken at a single time it is not always possible to positively identify separate mesoscale precipitation areas. This type of ambiguity is greatly reduced, however, when the areas are observed over a period of time. As they develop, move and dissipate, they can be recognized as individual entities. Subjectivity cannot be entirely eliminated from the analysis, but its influence on the results is not considered significant.

In the first study 8 LMSA's, 25 SMSA's and 125 cells were examined systematically. Areas, durations, motions and intensities of each were obtained from the radar PPI sequences. The intensities indicated by the radar were checked with those recorded by the gages. Vertical extent of cells and of the surrounding precipitation were observed on the RHI.

Fig. 2, an example of the data from the sensitive gage at the field station, shows the high degree of variability in rainfall rate as mesoscale areas and cells pass over the gage. Since the gage presents a one-dimensional cut of an irregular two-dimensional pattern, the mesoscale areas cannot be precisely and positively identified on the gage traces.

In the second study a single instantaneous precipitation pattern as depicted by the radar was analyzed in each of seventeen cyclonic storms. This approach, which permitted examination of a greater number of large mesoscale areas, was aimed toward obtaining a more complete description of the general configuration of LMSA's and of their distribution within the larger scale pressure and wind fields. Storms selected for this study were fully developed cyclones and were ones for which

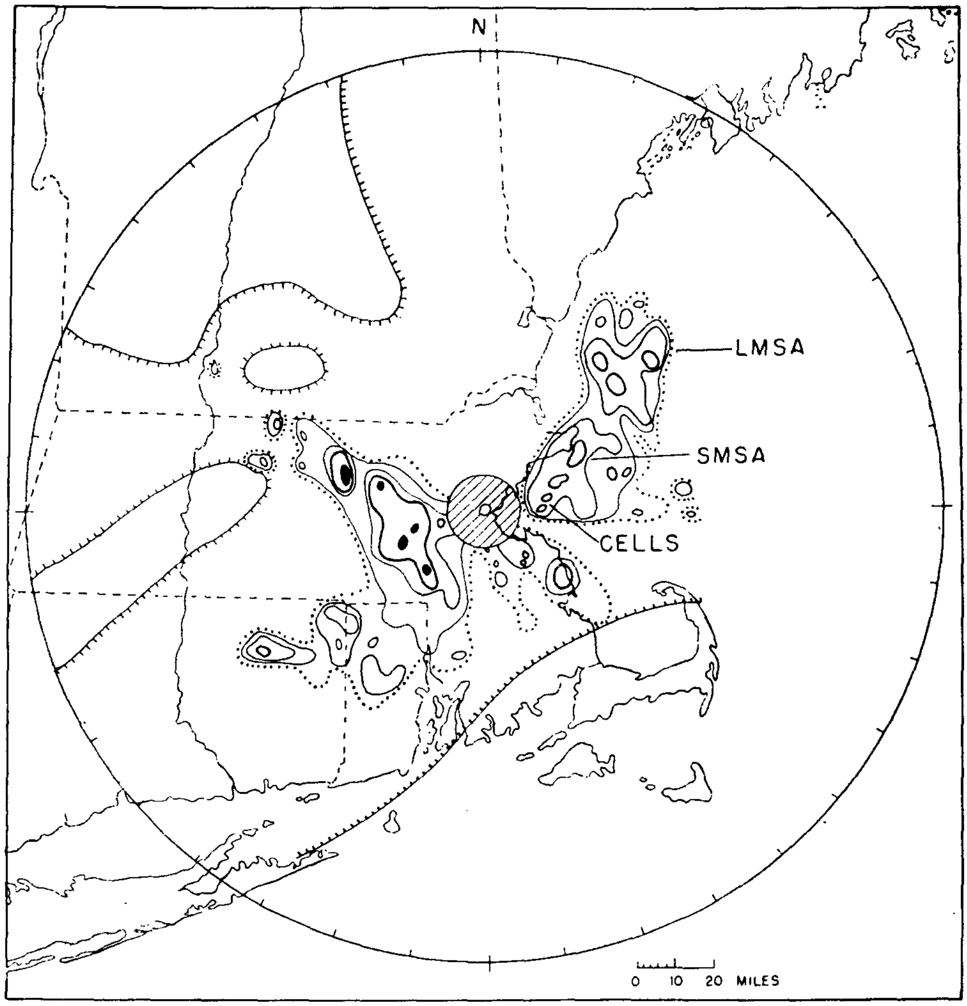

FIG. 1. Precipitation pattern showing large mesoscale areas (LMSA), small mesoscale areas (SMSA) and cells. Data taken with AN/CPS-9 radar, 8 July 1963, 0635 EST. Contours indicate equivalent rainfall rates: 0 (ticks), 1 (dotted), 2, 4, 8 and 16 (solid) mm hr^{-1}.

the radar and raingage records provided good coverage. Most of the data were taken with the WR-66 radar which shows the precipitation patterns clearly out to a range of 200 km. In the first study, range limitations in the radar data restricted rather severely the number of large mesoscale areas which could be analyzed in detail.

The shapes of precipitation areas were observed, and their orientations were compared with those of the surface isobars and with the surface wind direction during the hour sampled by radar.

3. Occurrence of precipitation areas of various scales

Each of the cyclonic storms (7 in the first group and 17 in the second) contained a synoptic precipitation area, but there were no synoptic rain areas associated with the frontal passage or air mass thunderstorms.

Within every synoptic precipitation area at least one LMSA was found, usually several. For the 17 cases in the second study, the number of LMSA's present at any one time within the radar circle, which is 200 km in radius, ranged from one to six; the observed distribution is shown in Fig. 3.

Within every large mesoscale area, both those in the synoptic precipitation areas and the frontal band which was *per se* a large mesoscale area, several small mesoscale areas were found. Also, with the exception of the air mass thunderstorms, which in themselves were separate small mesoscale areas, SMSA's rarely, if ever, were observed outside of the LMSA's. The number and concentration of small mesoscale areas within each large mesoscale area were recorded at several times and an average value of the number and density were noted. Results are in Table 2.

Cells were almost always located either within a clearly identifiable SMSA or in a cluster forming an area of similar size. At least one cell was found within each SMSA. The number and concentration of cells

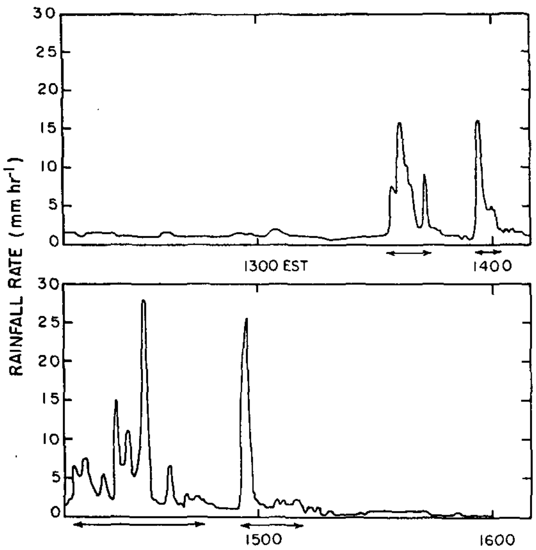

FIG. 2 Example of data from the high-resolution tipping bucket raingage, 29 August 1962. Small mesoscale precipitation areas (marked by arrows) are within a large mesoscale area which passed over gage between 1330 and 1515 EST. These data were taken on the southern extremity and late in the life history of the LMSA, so that the mesoscale rainfall rates are lighter than the typical ones given in Table 5.

within individual SMSA's were recorded at several times during their lifetimes and an average for each was obtained, the results being summarized in Fig. 4.

The basic pattern which was observed is that a precipitation area of any of the three sizes, synoptic, LMSA or SMSA, contains one or several of the next smaller-sized areas. It should be pointed out, however, that the structures are not rigid. The lifetimes of the smaller areas are considerably shorter than those of the larger ones. A synoptic area may last several days moving along with the cyclone; large mesoscale areas typically have lifetimes of several hours; small mesoscale areas an hour; and the duration of cells ranges from a few minutes to about half an hour. Therefore, the basic precipitation pattern continually changes texture as LMSA's build and dissipate within the synoptic areas, SMSA's build and dissipate within the LMSA's, and individual cells are relatively short-lived components of the SMSA's.

Similar behavior in precipitation patterns has also been observed in storms in other geographical areas.

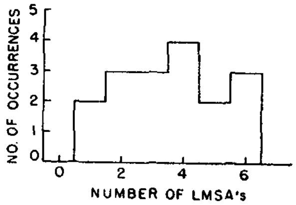

FIG. 3. Distribution of number of large mesoscale areas (LMSA's) appearing simultaneously in area observed by the radar, a circle with 200-km radius.

TABLE 2. The average number of SMSA's in each large mesoscale area at any one time, N_{SM}, and the average density of SMSA's per 2500 km² within each LMSA, D_{SM}.

	N_{SM}	D_{SM}
18 May 1963	3 4	2 4
8 July 1963 (PF)	3 4	2 3
8 July 1963 (F)	5	5
29 August 1962	5	3
17 September 1963	5 6	4 3

Browning and Harrold (1969) studied in detail the precipitation pattern within a wave depression which passed over Great Britain. Within this disturbance, they found generally band-shaped areas with widths of 50–100 km and lengths of 300–900 km; within the bands there were more intense "small areas" of the order of 1500 km²; clusters of cells were located within the "small areas." Matsumoto *et al.* (1967) in Japan and Elliott and Hovind (1964, 1965) in California found cumulus cells within disturbances of the size of large mesoscale areas, but did not mention whether they were further organized into smaller mesoscale areas. These findings suggest that precipitation patterns in New England and other regions have some similar mesoscale characteristics. However, in view of the differences in the convective instability of air masses influencing the climates of the different regions, the cumulus phenomena may be less extensively observed in general over Great Britain or on the west coast of the United States.

4. Characteristics of cells

Horizontal dimensions of the cells could not be determined because they often appeared to be at least

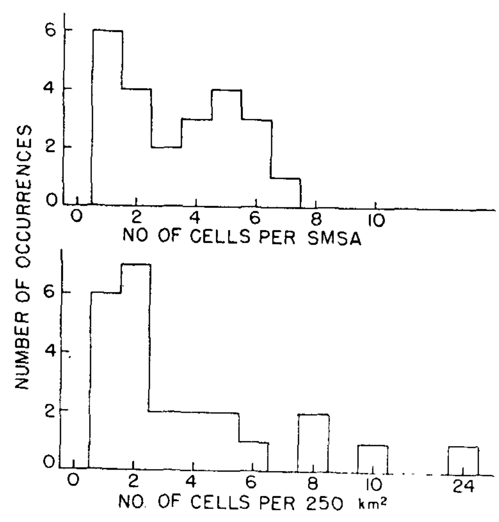

FIG. 4. Distribution for average number at one time and density of cells within the small mesoscale areas.

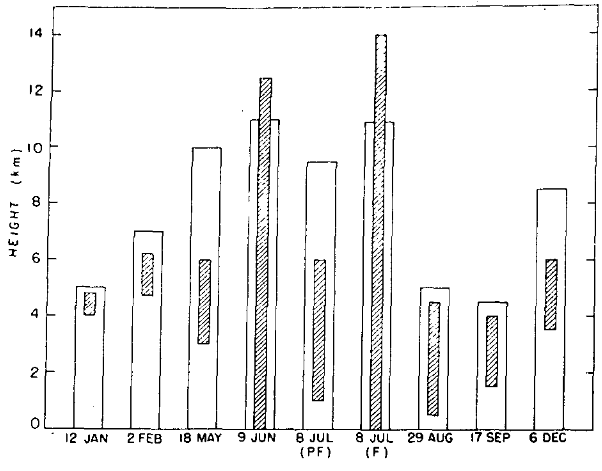

FIG. 5. Average vertical extent of cells (shaded portion) and of surrounding precipitation during each storm.

as small as the radar beam dimensions, but vertical extents were observed on the RHI by viewing cells at close ranges. In any single storm the cells tended to be of roughly the same depth at their maximum development, but the depths of the cells and the position of the layer containing them varied considerably from storm to storm. Vertical extent of cells and height of the surrounding precipitation for each of the storms are shown in Fig. 5. In summer showers and thunderstorms the cells appeared to extent throughout the depth of the surrounding precipitation and protruded above, while in the cyclonic storms they seemed to be completely embedded in the more widespread rain.

Fig. 6 shows distributions of the durations of cells measured in several storms. The distribution for 6 December 1962 is typical of the three winter storms in which most of the cells lasted only a few minutes. In cyclonic storms in other seasons there were also very many cells with only a few minutes' duration, but the distribution is broader, as on 17 September 1963. In the two storms which were composed of summer showers and thunderstorms, cell lifetimes were usually between 15 and 25 min with very few shorter than 10 min or longer than 30 min, as shown by the distribution for 9 June 1965.

The duration, depths and intensities of cells were more or less linearly related, as indicated in Fig. 7. Each

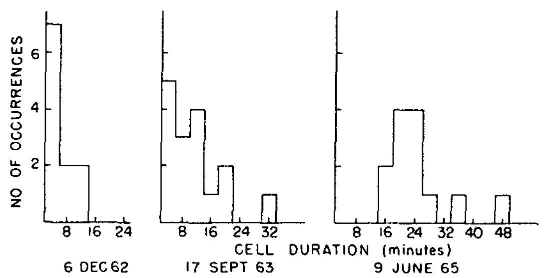

FIG. 6. Examples of distributions of the durations of cells for individual storms.

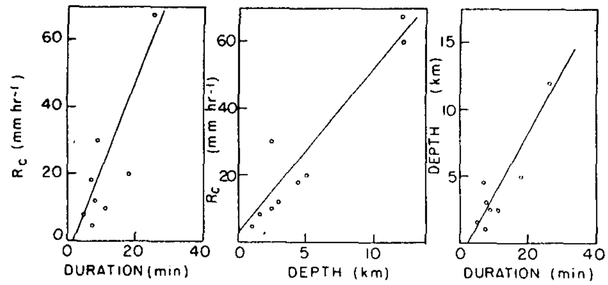

FIG. 7. Relations between depth, duration and rainfall intensity R_c for cells. Each point represents average values for all cells in one storm.

of the points in the figure represents one storm, showing the average values for the cells observed in that storm. The lines of best least-square fit indicate that the cells tend to last about 5 min for every 2 km of height and for each 12 mm hr^{-1} of rainfall rate. These results are in general agreement with the measurements of Battan (1959) who found similar durations for echoes from single-celled thunderstorms and a roughly linear relation between the areas and durations of the echoes.

The motions of cells observed from the radar were compared with the winds at the level midway between the top and bottom of the cells. Because of their short duration, cell motions were sometimes difficult to determine and in some of the storms appeared quite variable. The average velocities in each storm, however, were roughly in agreement with the wind flow at the mid-cell level, within $\pm 25°$ in direction and $\pm 50\%$ in speed in all cases, and generally much closer.

5. Small mesoscale areas

For each of the 24 small mesoscale areas, the average area was computed from a number of individual observations during its lifetime, the values being given in Fig. 8. The majority were between 100 and 400 km^2, with occasional larger ones up to 800 km^2. Durations could be observed for only 15 of the SMSA's; for the other nine, either the data were interrupted or the areas moved out of range. The durations, given in Table 3, varied from 20–150 min, the median value being 50 min.

During the lifetime of a mesoscale area, its shape changes continually. Therefore, its observed motion is not a simple translation; rather, it is the average rate of displacement of a continuously identifiable region of high reflectivity (relative to its immediate environment)

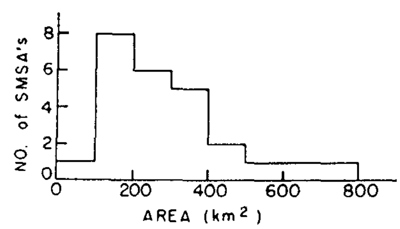

FIG. 8. Distribution of areas of small mesoscale areas.

TABLE 3. Duration (min) of small mesoscale areas.

Time interval	Number of SMSA's
>20	0
20–39	4
40–59	5
60–79	2
80–99	2
100–119	
120–139	
140–159	2

during the period when it could be clearly distinguished. With the exception of the thunderstorm complex, the motion of each SMSA appeared to be approximately the same as that of the cells within it, again within ±25° in direction and ±50% in speed. The thunderstorm complex of 9 June 1965 moved in a direction 45° to the right of the cell velocities.

6. Large mesoscale areas

Although large mesoscale precipitation areas were recognizable in all of the storms in the first study except for the thunderstorm complex, only a few could be identified and followed for a sufficiently long time to determine average areas, durations and motions. For these the average areas and durations are in Table 4.

Of the eight LMSA's observed in the first study, six were irregular in shape and were altering continuously during their lifetimes; their observed motions appeared to be about the same as those of the small mesoscale areas within them. Two of the LMSA's were definitely band-shaped, the frontal band on 8 July 1963 and one in the storm of 29 August 1962 which was an ex-hurricane. The motion of the band-shaped LMSA's appeared very slow and almost perpendicular to the motions of the SMSA's and cells within them.

The second study was undertaken to explore the general configuration of the larger mesoscale areas. Instantaneous precipitation patterns were used, so that durations and motions were not investigated. The seventeen cases which were selected were from fully developed cyclones prior to any occlusion; they represented a variety of positions of the observed precipitation area relative to the cyclone center and the surface fronts, as shown in Fig. 9. The precipitation pattern and the surface isobars and wind vectors, in Fig. 10, illustrate well the results which were obtained. In all of the cases elongated rain areas or band-shaped structures were observed. Many of these bands were similar in size to the large mesoscale areas examined in the first study but some were considerably larger, ranging up to 2×10^4 km^2 in extent. As pointed out earlier, it is not obvious, unless their life histories are studied, whether areas such as those marked A and B in Fig. 10 should be considered one LMSA or two. It is probable, therefore, that some of the bands observed in the second study consisted of two or more irregularly shaped LMSA's which formed an elongated rain area. In any case, the tendency to form elongated areas is very clear as demonstrated by the measured ratios of width to length in Fig. 11. It may be noted that in the cyclonic storm analyzed by Browning and Harrold (1969) the rain patterns also exhibited banded structures.

TABLE 4. Average areas (km^2) and durations (min) of large mesoscale precipitation areas.

Date	Area	Duration*
18 May 1963	3000 2200	200 240
8 July 1963 (PF)	3000 3300	80 >80
8 July 1963 (F)	2500	720
29 August 1962	4000	240
17 September 1963	3300 4500	>210 >210

* Durations preceded by > could not be determined more precisely because the data were interrupted.

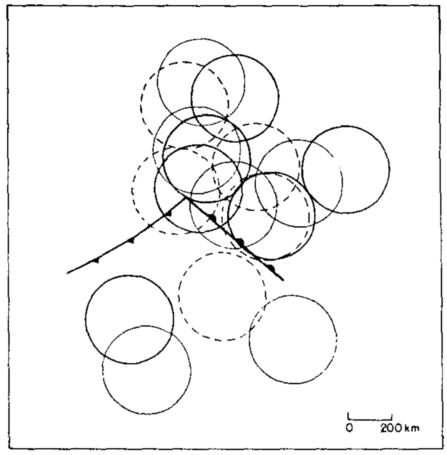

FIG. 9. Locations of the area observed by the radar relative to cyclone center and fronts for seventeen precipitation patterns analyzed in second study. All of the circles represent the same radar site relative to different storms. Light, heavy and dashed lines are used to make the circles more easily distinguishable.

The orientation of the bands were roughly parallel to the surface isobars. This is particularly noticeable in Fig. 10 where the cyclone center was within the region viewed by the radar and the structure bears some resemblance to the spiral bands in a hurricane. The distributions of orientation relative to surface isobars and surface wind direction is shown in Fig. 12; it can be seen that the angle between the band orientation and that of the isobars rarely exceeded 30°.

Both of these studies indicate rather clearly the existence of large mesoscale areas which contain small mesoscale areas and cells. But the evidence with respect to their areas, shapes and motions is somewhat inconclusive. In the first study the sample was very limited but the storms represented a variety of situations; in the second, the storms were all cyclones at roughly the

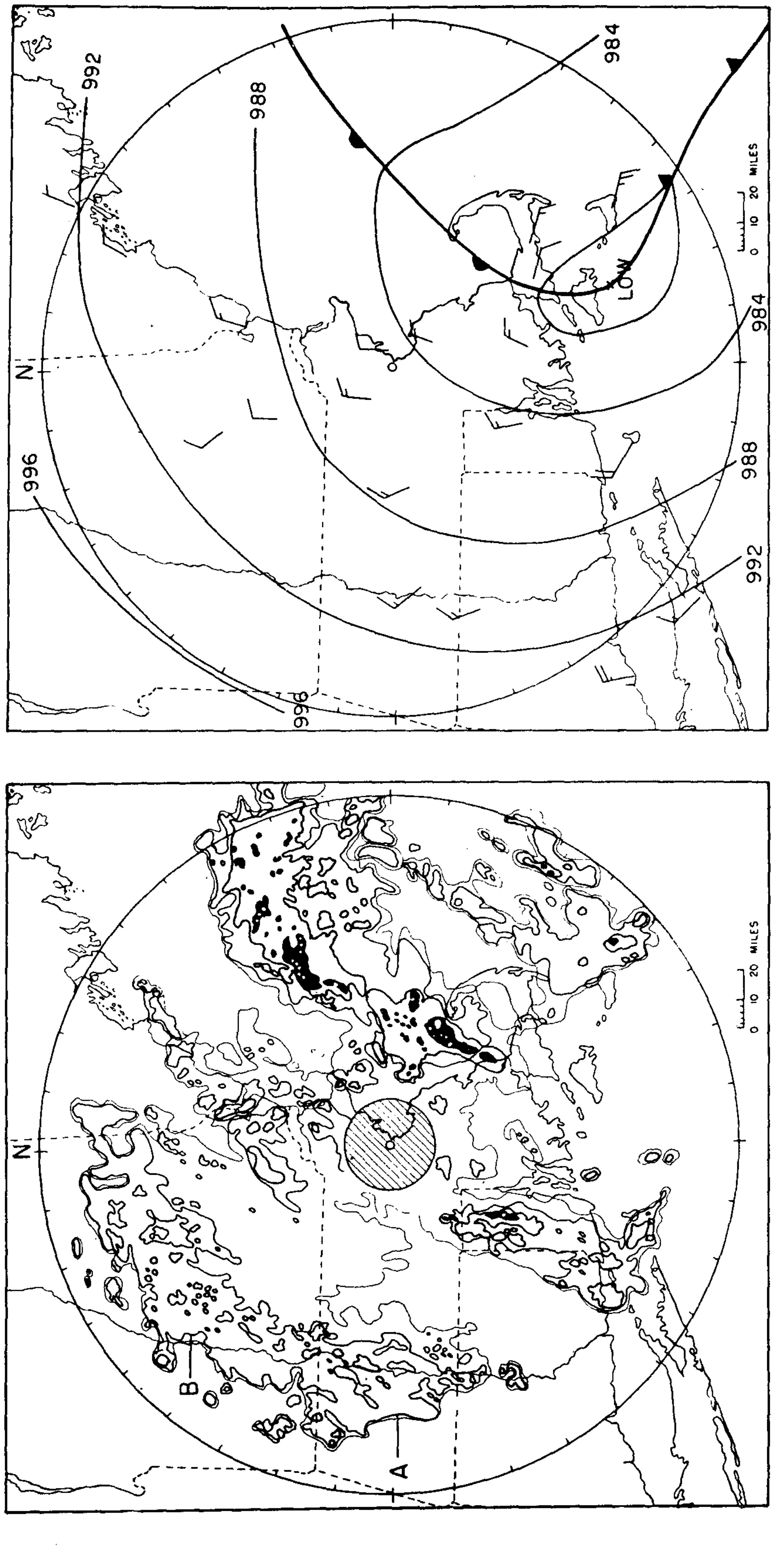

FIG. 10. Precipitation pattern, as depicted by WR-66 radar, and surface winds (kt) and isobars for 5 November 1969, 1300 EST. Contours represent the following values of equivalent rainfall rate: 2, 4, 8, 16 (solid black) and 32 (white spots) mm hr^{-1}.

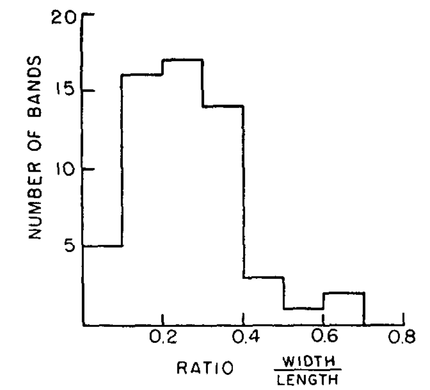

FIG. 11. Distribution of elongation of banded structures formed by large mesoscale areas.

same stage of development, and they showed similar pattern characteristics. More comprehensive analysis is needed before the average areas, motions and durations of the large mesoscale areas are fully described.

7. Intensity of precipitation in areas of various scales

Precipitation rates within the various areas, as determined from the radar and raingage data, are summarized in Table 5. Although the rainfall rates within the mesoscale areas varied considerably from day to day, on any given day, the variations were generally slight except in the frontal band and thunderstorm case. The ratios were about the same in all of the storms with R_{LM} being 2–4 times as great as R_S and R_{SM} about twice as large as R_{LM}. The rates in the cells varied more widely with R_C/R_{SM} ranging from 2–10.

The rate at which water was deposited by areas of each scale was computed from their observed rainfall rates and their average areas during the lifetime of each mesoscale area. In these computations an area of 8 km^2 was assigned to each cell. The results are in Table 6; it is evident that of the total water deposited by the large mesoscale areas, significant fractions come from each of the small and large mesoscale regions, while the cellular contribution ranged from 2–35%.

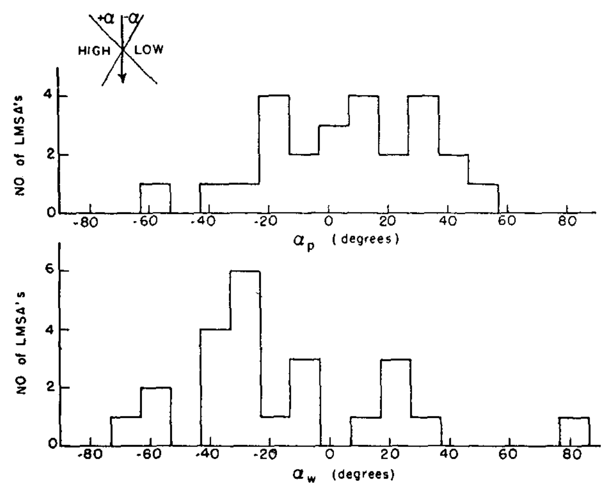

FIG. 12. Orientation of elongated rain areas relative to surface isobars, α_p, and to surface wind direction, α_w.

TABLE 5. Rainfall rates (mm hr^{-1}) for synoptic-scale precipitation areas (R_S), large mesoscale areas (R_{LM}), small mesoscale areas (R_{SM}), and cells (R_C) in each storm.

Date	R_S	R_{LM}	R_{SM}	R_C
12 Jan 63	0.5	*	1–2	2–4
2 Feb 63	0.5–1	*	2–3	5–10
18 May 63	0.2–0.5	2–3	5	10–15
9 Jun 65	0	0	5–20	45–90
8 Jul 63 (PF)	0.5–1	2	5	10–40
8 Jul 63 (F)	0	0.5–5	5–25	20–100
29 Aug 62	0.5–2	5	10	15–20
17 Sep 63	trace	0.5–1	2	4–15
6 Dec 62	0.5–1	*	3–6	10–50

* Not possible to determine.

8. Comments on the nature of mesoscale precipitation areas

Observations of the characteristics of mesoscale precipitation areas, both small and large, invite consideration concerning the physical bases for their occurrence since they represent a departure from the conventionally recognized "stratiform" and "convective" types of precipitation which are associated with synoptic- and cumulus-scale lifting, respectively.

One of the most notable features of the small mesoscale areas is an apparently close relationship with the convective cells, shown by the facts that every SMSA contained at least one cell and that their motions were very similar to those of the cells within them. An hypothesis which may be advanced is that much of the precipitation in the SMSA's is actually formed in cumulus updrafts and is spread by divergence aloft or simply left as cloud when the updraft dies. As pointed out by Houghton (1968) cumulus updrafts are generally of short duration and have a low precipitation efficiency. During the time that the updraft is active, water is condensed out rather rapidly in a region of limited horizontal extent. When the updraft dies much of the

TABLE 6. Water deposited by various parts of the larger mesoscale areas. Subscript LM denotes region in LMSA's but outside of SMSA's; SM is in SMSA's but outside of cells, and C denotes within cells.

Date	Total for LMSA (10^7 m^3 hr^{-1})	Percent in each area P_{LM}	P_{SM}	P_C
18 May 63	10.4	52	42	6
	7.1	33	65	2
8 Jul 63 (PF)	10.4	51	44	5
	15.7	27	48	25
8 Jul 63 (F)	31.2	11	54	35
29 Aug 62	32.7	22	69	9
17 Sep 63	2.8	37	42	21
	3.4	29	55	16

rain falls out quickly forming the sharp showers we call cells, but leaving considerable amounts of condensate aloft as cloud or small precipitation particles which fall slowly and may have been spread by divergence over a larger area. If several updrafts or cells form close to each other either simultaneously or in a sequence, the condensate which they leave aloft would accumulate to create a small mesoscale precipitation area which would last as long as cells continue to develop within it but would rain out and disappear shortly after the cessation of convective activity. This hypothesis is supported by the results of Melvin (1968) who, using quantitative radar displays, examined six thunderstorm complexes for their entire lifetimes and also a developing squall line. He found that the precipitation areas appeared to develop around the cells and lasted only as long as cells continued to form. He also computed the updraft velocities which would be required to produce the condensate for the observed precipitation and for various assumed values of the efficiency of precipitation; the resulting values appeared quite reasonable.

Qualitatively, this hypothesis appears plausible for small mesoscale areas in cyclonic storms also. If cells are imbedded in more widespread precipitation, any condensate which is not deposited in the resulting shower would be added to the general rain forming a small mesoscale area around a group of showers. At least one cell was observed in every SMSA; but in some of them, for example 18 May 1963, the percentage of rain in the cells is extremely small compared with that in the small mesoscale areas, and some other mechanism may be involved.

With regard to the large precipitation areas, we note that in their general configuration they appear to be more closely related to the features of the synoptic maps than to those of the smaller-scale rain areas within them. An understanding of the nature of this relationship and the basis for the strong tendency to form banded structures must await a more detailed study of the life histories of these areas.

9. Conclusion

The results which have been presented are based on a rather small sample because detailed analysis of cells and mesoscale precipitation areas from photographs of radar displays is extremely time-consuming. In spite of its small size, however, the sample contains a wide variety of storm types and in all of them the precipitation patterns, which initially appeared very dissimilar, turned out to be composed of subsynoptic-scale precipitation areas with rather clearly definable characteristics and behavior.

The consistent occurrence of subsynoptic-scale rain areas with similar characteristics and behavior of precipitation patterns makes it possible to describe the distribution of precipitation in any storm in a parameterized manner by giving the number, intensities, height, and horizontal extent of precipitation areas of each scale. Such a description is comparable in resolution to that provided by point-by-point intensity values every kilometer or two, but it is clearly much more compact and is also more informative since it identifies and emphasizes the basic features of the pattern.

Realistic models of storms which include these basic features in typical configurations can be used to study the precipitation mechanisms on the various scales and to explore indirectly the subsynoptic-scale atmospheric motions associated with them. This last point is of especial importance because direct investigation of small-scale phenomena by analysis of measured values of wind, temperature, humidity and pressure is usually not feasible because of the density of the observational network required.

Clearly it would be desirable to find a more objective mode of defining and identifying mesoscale precipitation areas than has been achieved in this study. If their characteristics could be analyzed by computer techniques much more data could be handled, and more comprehensive statistics would emerge. The intricate texture of the patterns, however, with areas of each scale containing several of the next smaller scale, poses rather stringent requirements on the resolution both spatially and with respect to signal intensity. Efforts to deduce statistical properties of weather radar echoes from digitized data (for example, Kessler and Russo, 1963) have not proved very fruitful, probably because the resolution was inadequate and the analysis was geared to a simpler type of structure than actually occurs in nature.

Future research will be directed toward obtaining more definitive characterization of the large mesoscale areas and toward development of kinematic models for interpreting precipitation patterns in terms of the subsynoptic motions which produce them. Efforts will also continue toward finding objective numerical methods for analyzing radar observations of subsynoptic-scale precipitation areas.

Acknowledgments. The research reported in this paper was performed under National Science Foundation Grant GA-10420.

REFERENCES

Battan, L. J., 1959: *Radar Meteorology*. The University of Chicago Press, p. 83.

Browning, K. A. and T. W. Harrold, 1969: Air motion and precipitation growth in a wave depression. *Quart. J. Roy. Meteor. Soc.*, **95**, 288–309.

Elliott, R. D., and E. L. Hovind, 1964: On convection bands within Pacific coast storms and their relation to storm structure. *J. Appl. Meteor.*, **3**, 143–154.

——, and ——, 1965: Heat, water, and vorticity balance in frontal zones. *J. Appl. Meteor.*, **4**, 196–211.

Houghton, H. G., 1968: On precipitation mechanisms and their artificial modification. *J. Appl. Meteor.*, **5**, 851–859.

Kessler, E., III, and J. A. Russo, Jr., 1963: Statistical properties of weather radar echoes. *Preprints of Papers, Tenth Wea. Radar Conf.*, Amer. Meteor. Soc., pp. 25–33.

Matsumoto, S., K. Ninomiya and T. Akiyama, 1967: A synoptic and dynamic study on the three-dimensional structure of mesoscale disturbances observed in the vicinity of a cold vortex center. *J. Meteor. Soc. Japan*, **45**, 64–81.

Melvin, G. L., 1968: The development of thunderstorm complexes and their associated vertical transports. S.M. thesis, Department of Meteorology, M. I. T.